

# Understanding Floquet Resonances in Ultracold Gas Scattering

Christoph Dauer, Axel Pelster<sup>✉</sup>, and Sebastian Eggert<sup>✉</sup>  
*Physics Department and Research Center OPTIMAS,  
 RPTU Kaiserslautern-Landau, 67663 Kaiserslautern, Germany.*  
 (Dated: March 4, 2025)

Scattering by a short-range potential with time-periodic interaction strength is investigated with a Floquet-scattering theory. Sharp resonances occur, at which the s-wave scattering length can be tuned to large positive and negative values. We show that the shape of these resonances is described by a simple formula, and find that both resonance position and prefactor can be altered by the driving strength. Our approach allows to identify the physical origin of the scattering resonances as Floquet bound states with positive energies, which are dynamically created by the drive. This insight is valuable for a detailed analysis and uncovers a general resource for enhanced or reduced scattering in Floquet systems.

The understanding of interaction effects in quantum systems remains a major challenge in many fields of physics. In this context *tunable* interactions are extremely valuable for systematic studies of correlated many-body phenomena. Accordingly, extensive research has focused on adjustable scattering lengths in ultra-cold quantum gases, using Feshbach resonances [1–5], near resonant light [6–11], and microwave fields [12–20].

We now examine the possibility of using time-periodic scattering lengths as an additional tuning mechanism [17, 19, 20]. Time-oscillating lattices and interactions are known as Floquet systems and have been proposed and used in a large variety of setups [21–49]. For a one-dimensional setup it is known that a Floquet impurity potential can have a rather dramatic effect [50–52]: even an infinitesimally small driving amplitude can completely block one-dimensional transport at special resonances. Such a quantum resonance catastrophe has great potential for magnetic filters [52] and superconducting filters [53, 54]. Very recently, time-oscillating interparticle potentials were experimentally analyzed using ultra-cold <sup>6</sup>Li atoms [20], realizing the effect of a "Floquet-Feshbach resonance" with the help of an oscillating magnetic field [17, 19]. In this work we now seek to uncover the physical origin of such resonances from general time-periodic interactions and provide closed formulas for the effective scattering, which will be analyzed to give straightforward analytic predictions for the locations and prefactors of the resonant behavior. We also predict a small imaginary part corresponding to losses into higher frequency modes.

The proposed setup can be modeled by a time-periodic s-wave scattering length

$$a(t) = \bar{a} + a_1 \cos(\omega t), \quad (1)$$

where the amplitude is assumed to fulfill the restriction  $|a_1| < |\bar{a}|$ . In the center-of-mass frame of reference the s-wave collisions of ultracold atoms are described by the Hamiltonian

$$H(r, t) = \frac{\hbar^2}{2\mu} \left[ -\Delta + 4\pi a(t) \delta^3(\mathbf{r}) \frac{\partial}{\partial r} r \right], \quad (2)$$

in terms of the short-range pseudo-potential formalism [55, 56] along the radial coordinate  $r$  with reduced mass  $\mu$ . No assumptions are made about the underlying mechanism for the oscillating modulation  $a(t)$ , but it is instructive to consider prototypical values corresponding to ultracold <sup>6</sup>Li atoms in a magnetic field [20]: The collision energy at  $T \sim 770$  nK is about a factor of 1000 smaller than the typical dimer energy  $E_{\bar{a}} = \hbar^2/2\mu\bar{a}^2 \approx 2\pi\hbar \times 16$  MHz at  $\bar{a} = 100$  Å. In the following we use units of  $\hbar = \hbar^2/2\mu = 1$ , i.e. measuring length scales in units of  $|\bar{a}|$  will result in energies and frequencies relative to  $E_{\bar{a}}$ .

For a time periodic Hamiltonian  $H = H_0 + H_1 \cos \omega t$  the steady states  $\psi(r, t) = e^{-i\epsilon t/\hbar} \phi(r, t)$  can be found by Floquet theory [57–61], where  $\epsilon$  is the Floquet eigenenergy. Using the Fourier transformation  $H_n = \int_0^T dt e^{in\omega t} H(t)/T$  and the time-periodic Floquet mode  $\phi(r, t) = \sum_n e^{-in\omega t} \phi_n(r)$ , the time-dependent Schrödinger equation becomes an eigenvalue equation for the Floquet quasi-energy  $\epsilon$

$$H_0 \phi_n(r) + H_1 [\phi_{n-1}(r) + \phi_{n+1}(r)]/2 = (\epsilon + n\omega) \phi_n(r). \quad (3)$$

In terms of the pseudo-potential from Eq. (2) this yields

$$(\Delta + \epsilon + n\omega) \phi_n = 4\pi \delta^3(\mathbf{r}) \frac{\partial}{\partial r} r (\bar{a} \phi_n + a_1 \frac{\phi_{n+1} + \phi_{n-1}}{2}). \quad (4)$$

We make the s-wave scattering ansatz

$$\phi_n(r) = \delta_{n,0} \frac{\sin k_0 r}{k_0 r} + f_n \frac{e^{ik_n r}}{r}, \quad (5)$$

with an incoming plane wave  $k_0$  in the  $n = 0$  channel. Note, that for  $r > 0$  the usual wave equation is fulfilled for each channel  $H_0 \phi_n = k_n^2 \phi_n = (\epsilon + n\omega) \phi_n$ , which fixes the Floquet energy  $\epsilon = k_0^2$  and all scattered wave vectors  $k_n = \sqrt{\epsilon + n\omega}$ . The scattering amplitudes  $f_n$  for  $n > 0$  correspond to open channels, where particles are lost, while  $n < 0$  are bound states which lead to interesting resonances as we will see below. Using  $\Delta \frac{1}{r} = -4\pi \delta^3(\mathbf{r})$

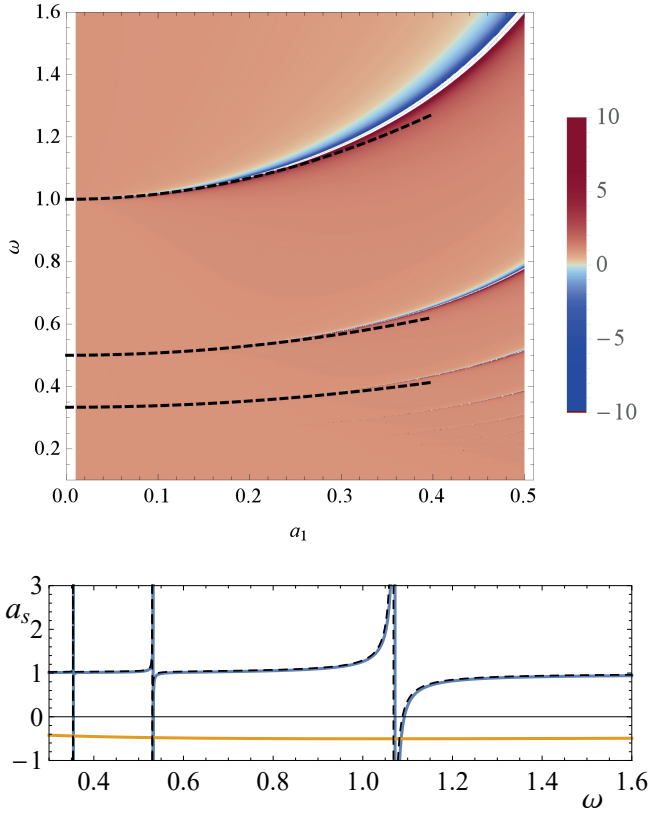


Figure 1. Results for  $a_s$  compared to the analytic prediction in Eqs. (17)–(20) (dashed) for  $\epsilon \rightarrow 0$ . Top: Real part as function of driving frequency  $\omega$  and amplitude  $a_1$ . Bottom: Imaginary part multiplied by 100 (orange) and real part (blue) for  $a_1 = 0.2\bar{a}$ .

we arrive at the recursion relation

$$k_n f_n = L_n (k_{n+1} f_{n+1} + k_{n-1} f_{n-1}) + h_n, \quad (6)$$

$$\text{where } L_n = -\frac{ia_1 k_n}{2(1 + i\bar{a}k_n)}, \quad (7)$$

$$h_n = -iL_n(2\delta_{n,0}\bar{a}/a_1 + \delta_{|n|,1}). \quad (8)$$

For a numerical analysis we could stop at this point since the linear set of Eq. (6) can be efficiently solved with the convergence condition  $f_{|n| \rightarrow \infty} \rightarrow 0$ . Interestingly, as shown in Fig. 1, large resonances are observed even for small  $a_1$  if  $\bar{a} > 0$  which we will analyze in the following.

First, we derive a continued fraction solution by dividing the recursion in Eq. (6) for  $|n| > 1$  by the left-hand side, so it can be expressed in terms of fractions  $g_n^\pm = k_n f_n / (L_n k_{n \mp 1} f_{n \mp 1})$  for positive  $n > 1$  and negative  $n < -1$ , respectively:

$$g_n^\pm = \frac{1}{1 - L_n L_{n \pm 1} g_{n \pm 1}^\pm} = \frac{1}{1 - \frac{L_n L_{n \pm 1}}{1 - \frac{L_{n \pm 1} L_{n \pm 2}}{1 - \frac{L_{n \pm 2} L_{n \pm 3}}{\dots}}}}. \quad (9)$$

Here, we have inserted the definition of  $g_n^\pm$  into Eq. (6) to obtain the relation in Eq. (9), which leads to the contin-

ued fraction solution by straight-forward iteration [62–64]. Inserting  $g_{\pm 2}^\pm$  from Eq. (9) into Eq. (6) for  $n=0, \pm 1$  the scattering amplitude is expressed in terms of an effective scattering length  $a_s$  (see End Matter A)

$$f_0 = -\frac{a_s}{1 + ik_0 a_s}, \quad (10)$$

$$\text{where } a_s = \bar{a} + a_1(L_1 g^+ + L_{-1} g^-)/2. \quad (11)$$

Here  $g^\pm = 1/(1 - L_{\pm 1} L_{\pm 2} g_{\pm 2}^\pm)$  are given by the continued fractions for  $n = \pm 1$  in Eq. (9). The effective scattering length  $a_s$  has two separate contributions from the periodic driving  $a_1$ . The term  $a_1 L_1 g^+$  from the open channels  $n > 0$  is of order  $a_1^2$  and has both real and imaginary parts. This is due to the fact that particles are scattered into higher energy Fourier modes and are considered lost. The term  $a_1 L_{-1} g^-$  from the closed channels  $n < 0$  is purely real since  $L_{n < 0} \in \mathbb{R}$  and shows pronounced divergences if  $\bar{a} > 0$ . In fact, the form of the parameters  $L_n$  in Eq. (7) indicate singular points for  $-i\bar{a}k_n = 1$ . Using  $k_n = \sqrt{n\omega + \epsilon}$ , resonances will therefore occur for negative  $n$  close to  $n\omega + \epsilon \sim -1/\bar{a}^2$  if  $\bar{a} > 0$ . Note, that for  $\bar{a} < 0$  no resonances are found. In the following, we assume positive scattering lengths and set  $\bar{a} = 1$ , so energies and frequencies are given in units of  $E_{\bar{a}}$ .

For the leading resonance and small  $a_1$  it is sufficient to keep only the first fraction of  $g^-$  in Eqs. (9) and (11). To order  $a_1^2$  the resonance is then determined by  $1 - L_{-1} L_{-2} = 0$  to be of the standard form [5]

$$a_s \approx 1 + \frac{\Delta_1}{\omega_1 - \omega}, \quad (12)$$

where in the low-energy limit  $\epsilon \rightarrow 0$  position and prefactor, i.e. width, read  $\omega_1 = 1 + (1 + 1/\sqrt{2})a_1^2$  and  $\Delta_1 = a_1^2/2$ , respectively. In addition we get an imaginary contribution  $\text{Im}(a_s) \approx -a_1^2 \sqrt{\omega}/(4 + 4\omega)$  from the open channels, which is typically much smaller than the background as shown in Fig. 1[Bottom]. Even though higher-order terms in  $a_1$  have been neglected, Eq. (12) gives quite accurate results even for an amplitude of 20% driving strength as can be seen in Fig. 1. Note, that both prefactor and frequency shift of the divergence scale with  $a_1^2$  up to higher-order corrections, which has been tested and confirmed in experiments [20]. The central result in Eq. (12) provides a quick and accurate prediction for location and strength of the leading resonance, which can be tuned by both amplitude and frequency. In Fig. 1 we plot the results in the low-energy limit  $\epsilon \rightarrow 0$  corresponding to the physical situation in ultracold gases where  $k_B T \ll \hbar\omega$  [20].

In order to unravel the physical origin of the resonances, we now propose an analysis in terms of Floquet bound states, which we define and predict below. It is well known that bound states are a valuable resource for strongly enhanced scattering resonances in the context of Feshbach resonances [1–5], Fano resonances [65, 66], or

bound states in the continuum [67, 68]. The mechanism for Floquet resonances is more involved, since in this case the bound state itself is generated dynamically, i.e. the periodic drive creates the bound state, tunes the resonance, and also provides the coupling, simultaneously.

Floquet bound states are defined as distinct solutions  $|\phi^m\rangle$ , labeled by the index  $m = 1, 2, 3, \dots$ , to the Schrödinger equation, where only negative Fourier modes  $n < 0$  are occupied. Using the Ansatz

$$\phi_n^m(r) = D_n^m \frac{e^{-\kappa_n^m r}}{\kappa_n^m r} \quad (13)$$

with  $\kappa_n^m = -ik_n^m = \sqrt{-\epsilon_m - n\omega}$  and the normalization condition  $\sum_{n<0} |D_n^m|^2 (\kappa_n^m)^{-3} = 1/(2\pi) = \mathcal{N}^2$  [69], we obtain from Eq. (4)

$$(1 - \kappa_n^m) D_n^m = \frac{a_1}{2} \kappa_n^m (D_{n-1}^m + D_{n+1}^m), \quad \forall n < 0, \quad (14)$$

$$\text{where } \lim_{n \rightarrow -\infty} D_n^m = 0 \text{ and } D_0^m = 0. \quad (15)$$

Note, that Eq. (14) corresponds to Eq. (6) for  $n < 0$  and  $D_n^m = \kappa_n^m f_n$ , but with the boundary condition  $\phi_0 = 0$ . Analogous to a static Schrödinger equation, a set of localized solutions  $|\phi^m\rangle$  can be found at discrete energies  $\epsilon_m(\omega)$  with  $m = 1, 2, 3, \dots$ , depending on frequency  $\omega$  and amplitude  $a_1$ . Floquet bound states exist without any incoming wave  $D_0^m = 0$  due to the periodic drive.

Before analyzing the corresponding eigenenergies  $\epsilon_m$  in detail below, let us consider the implications. The effect of bound states in the continuum on scattering resonances was discussed in a number of different un-driven systems [1–5, 65–68]. In the End Matter B we now present an explicit derivation of the effect of Floquet bound states, which follows a slightly different logic from the known static cases [1–5, 65–68]. As a result our theory accurately predicts all resonances in the effective scattering lengths in terms of the bound state energies  $\epsilon_m(\omega)$  and the first components  $D_{-1}^m$  of the normalized bound states  $|\phi^m\rangle$

$$a_s = 1 - \sum_m \frac{\pi a_1^2 |D_{-1}^m|^2}{\epsilon_m - \epsilon} + a_1 L_1 g^+ / 2. \quad (16)$$

This central result uncovers the physical origin of the observed resonances quantitatively in terms individual bound state solutions. Note, that the locations of the resonances are given by  $\epsilon = \epsilon_m$ , which are relevant if the bound state energies are positive, i.e. they represent bound states in the continuum [67, 68]. Expanding the frequency dependence to linear order around the incoming energy  $\epsilon_m \approx \epsilon + (\omega - \omega_m) \partial_\omega \epsilon_m$  for each  $m$  yields the standard form of the resonances analogous to Eq. (12)

$$a_s \approx 1 + \sum_m \frac{\Delta_m}{\omega_m - \omega} \quad (17)$$

with identifying  $\Delta_m = \pi a_1^2 |D_{-1}^m|^2 / \partial_\omega \epsilon_m$ , where the open-channel contribution  $a_1 L_1 g^+ / 2$  has been omitted. By numerically solving the Floquet bound states, we have tested and confirmed that the predicted positions of the resonances in Eqs. (16) and (17) agree exactly with the continued fraction solution. We now proceed to find analytic approximations for  $\omega_m$  and  $\Delta_m$ , which can be used for closed form quantitative predictions, that are plotted as dashed lines in Fig. 1 and Fig. 2.

For small  $a_1$  a perturbative analysis of the bound-state solutions can be used for Eq. (14). To zeroth order in  $a_1$  in Eq. (14) the energies are found by  $\kappa_n^m = 1$ , which is fulfilled for discrete zeroth order energies  $\epsilon_m = -1 + m\omega$  and zeroth-order eigenstates  $D_n^m = \mathcal{N} \delta_{m,-n}$ . It may be surprising that bound states are predicted in zeroth order, i.e. for zero amplitude driving, but it is correct in the sense that resonances exist in the limit of infinitesimally small  $a_1$  at frequencies  $\omega_m = (1 + \epsilon)/m$ . The zeroth order location of the resonances depend on the incoming energy  $\epsilon$  and the order  $m$ , but remarkably the resonant bound wave-function has the universal form  $\mathcal{N} e^{-r}/r$  from Eq. (13) due to the underlying condition  $\kappa_n^m = 1$ , i.e. the size is always given by the average scattering length  $\bar{a}$ .

Next, we turn to the first-order correction in  $a_1$  which yields the neighboring coefficients  $D_{\pm 1 - m}^m = \mathcal{N} a_1 / (2 / \kappa_{\pm 1 - m}^m - 2)$ . Here we inserted the zeroth order solution  $D_{-m}^m = \mathcal{N}$  into Eq. (14) for  $m = -n \pm 1$  and used  $\kappa_{\pm 1 - m}^m = \sqrt{1 \mp \omega}$ . Finally, the second-order correction follows from Eq. (14) for  $m = -n$

$$\frac{1}{\sqrt{m\omega - \epsilon_m}} - 1 \approx \frac{a_1^2}{4} \left( \frac{\sqrt{1 + \omega}}{1 - \sqrt{1 + \omega}} + \frac{\sqrt{1 - \omega}}{1 - \sqrt{1 - \omega}} \right). \quad (18)$$

Solving this equation for  $\omega_m$  with the resonance condition of incoming energy  $\epsilon = \epsilon_m = 0$  gives all positions of the resonances up to order  $a_1^2$

$$\omega_m \approx \frac{1}{m} + \frac{a_1^2}{2m} \left[ 2 + \sqrt{m(m+1)} - \sqrt{m(m-1)} \right] \quad (19)$$

in the limit  $k_0 \rightarrow 0$  in agreement with recent experiments [20]. The leading order of the respective prefactors of the divergences as a function of  $a_1$  results to [70]

$$\Delta_m = \frac{a_1^{2m}}{2^{2m-1} m} \prod_{j=1}^{m-1} \left( \frac{1}{\sqrt{1 - j\omega_m}} - 1 \right)^{-2}. \quad (20)$$

in good agreement with the full solution in Fig. 1 for  $a_1 = 0.2$ . Since  $\Delta_m \propto a_1^{2m}$  becomes very small for higher orders  $m > 1$ , we also we need to consider stronger amplitudes beyond the perturbative approach.

Approaching larger  $a_1 \rightarrow \bar{a}$  it turns out that the differences between neighboring coefficients in Eq. (14) rapidly become smaller, so that a continuous description in terms of differential equations can be used for the recursion relation. The details are presented in End Matter C with

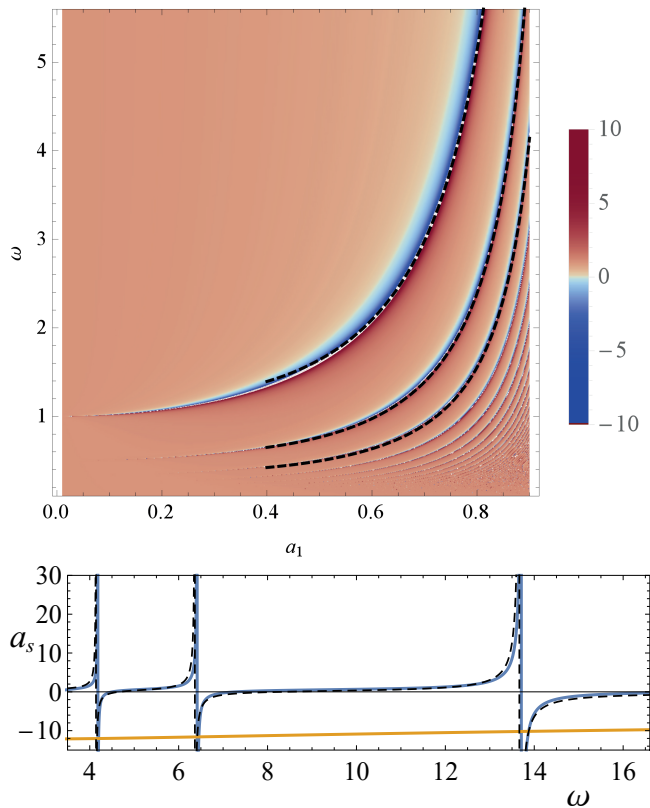


Figure 2. Results for  $a_s$  compared to the analytic prediction (black dashed) in Eqs. (17), (34), and (35) for  $\epsilon \rightarrow 0$ . Top: Real part as function of frequency and amplitude. Bottom: Imaginary part multiplied by 100 (orange) and real part (blue) for  $a_1 = 0.9\bar{a}$ .

the outcome in Eq. (34) that the resonance positions diverge in the limit  $a_1 \rightarrow \bar{a}$  according to

$$\lim_{a_1 \rightarrow \bar{a}} \omega_m \propto \frac{1}{\sqrt{a_1(1-a_1)^3}}. \quad (21)$$

The proportionality constants are given in the End Matter C as well as the corresponding expression for  $\Delta_m$  in Eq. (35). This results in the dashed lines in Fig. 2 in good agreement with the exact solution.

Analytical results are also possible in the limit of large frequencies  $\omega \gg \omega_1 > E_{\bar{a}}$  in a regime that is beyond any resonance. In the recursion relation  $|k_n| \rightarrow \infty$  for  $n \neq 0$  in Eq. (7) leads to coefficients  $L_n \rightarrow -a_1/(2\bar{a})$  independent of  $n$ . Therefore, also the continued fraction in Eq. (9) becomes independent of  $n \neq 0$  and can be solved by a quadratic equation  $g_n^\pm \rightarrow \frac{2\bar{a}^2}{a_1^2}(1 - \sqrt{1 - a_1^2/\bar{a}^2})$ . Inserting this into Eq. (11) we have

$$\lim_{\omega \rightarrow \infty} a_s = \bar{a} \sqrt{1 - \frac{a_1^2}{\bar{a}^2}}. \quad (22)$$

Hence, even for very large frequencies the driving does not average out, but reduces the magnitude of the effective scattering length. Note, that the result in Eq. (22)

is not limited to small  $a_1$  or positive  $\bar{a}$ . It implies that the effective interaction can be reduced by high frequency driving, but never outside the range  $\bar{a} \pm a_1$  of the time-dependent scattering in Eq. (1). In the high-frequency limit, the behavior of experimental systems is typically stable over longer time-scales, since there are no resonances and the losses become negligible. Hence, the result in Eq. (22) is suitable to be tested experimentally.

Last but not least, let us discuss the effects of higher harmonic terms in the time-dependence of Eq. (1) with integer multiples of  $\omega$ . This may be relevant in case the scattering length is modified using a field in Feshbach resonance  $a(t)/a_{\text{bg}} = 1 - \Delta/[B(t) - B_0]$  beyond a linear regime, but may also offer more tuning possibilities. The time-dependence of the underlying field is normally under good control, so a perfect harmonic drive can be realized, as well as large higher harmonic contributions. Since the Hamiltonian is still time-periodic, the Floquet approach remains possible and the recursion relation can be modified in a straight-forward way. Preliminary numerical results show that the principle structure of strong resonances is quite robust in the presence of higher harmonics, but changes quantitatively. This is also true for the imaginary part, which may be larger but may also be strongly suppressed. For a suppression, the phase and amplitude of the higher harmonics must be tuned so that the higher order amplitudes  $f_{n>0}$  are very small, which is feasible in experiment [20]. However, finding a general protocol to achieve this effect was so far not possible. We should mention at this point that an analysis of higher angular momentum Floquet scattering is also possible [70], in case larger energies become relevant.

In summary, we have analyzed the effect of a time-periodic scattering length in interacting many-body systems. The resulting effective scattering amplitude is highly tunable by the frequency and the amplitude of the drive. In particular, a strong sharp enhancement is possible using even quite small amplitudes, which has great potential for future applications. A closed form of the scattering amplitude was derived and analyzed, resulting in quantitative predictions for the locations and widths of resonances. Equally important, we uncovered the underlying mechanism of the strong resonance behavior, namely bound Floquet states with positive energies, which are created dynamically by the drive. This insight has proven to be valuable for obtaining analytic predictions, but also opens the door for a systematic search, analysis, and creation of such bound Floquet states in related systems for enhanced tuning possibilities, changing interactions from small to large values with slight parameter changes.

## ACKNOWLEDGEMENT

We thank A. Guthmann and A. Widera for inspiring discussions. Furthermore, we acknowledge financial support by the Deutsche Forschungsgemeinschaft (DFG, German Research Foundation) via the Collaborative Research Center SFB/TR185 (Project No. 277625399).

- 
- [1] S. Inouye, M. R. Andrews, J. Stenger, H.-J. Miesner, D. M. Stamper-Kurn, and W. Ketterle, “Observation of Feshbach resonances in a Bose-Einstein condensate,” *Nature* **392**, 151 (1998).
- [2] E. Timmermans, P. Tommasini, M. Hussein, and A. Kerman, “Feshbach resonances in atomic Bose-Einstein condensates,” *Phys. Rep.* **315**, 199 (1999).
- [3] V. Vuletić, A. J. Kerman, C. Chin, and S. Chu, “Observation of low-field Feshbach resonances in collisions of Cesium atoms,” *Phys. Rev. Lett.* **82**, 1406 (1999).
- [4] C. Chin, V. Vuletić, A. J. Kerman, and S. Chu, “High resolution Feshbach spectroscopy of Cesium,” *Phys. Rev. Lett.* **85**, 2717 (2000).
- [5] C. Chin, R. Grimm, P. Julienne, and E. Tiesinga, “Feshbach resonances in ultracold gases,” *Rev. Mod. Phys.* **82**, 1225 (2010).
- [6] P. O. Fedichev, Y. Kagan, G. V. Shlyapnikov, and J. T. M. Walraven, “Influence of nearly resonant light on the scattering length in low-temperature atomic gases,” *Phys. Rev. Lett.* **77**, 2913 (1996).
- [7] R.A. Duine and H.T.C. Stoof, “Atom–molecule coherence in Bose gases,” *Phys. Rep.* **396**, 115 (2004).
- [8] M. Theis, G. Thalhammer, K. Winkler, M. Hellwig, G. Ruff, R. Grimm, and J. Hecker Denschlag, “Tuning the scattering length with an optically induced Feshbach resonance,” *Phys. Rev. Lett.* **93**, 123001 (2004).
- [9] G. Thalhammer, M. Theis, K. Winkler, R. Grimm, and J. Hecker Denschlag, “Inducing an optical Feshbach resonance via stimulated Raman coupling,” *Phys. Rev. A* **71**, 033403 (2005).
- [10] T. L. Nicholson, S. Blatt, B. J. Bloom, J. R. Williams, J. W. Thomsen, J. Ye, and P. S. Julienne, “Optical Feshbach resonances: Field-dressed theory and comparison with experiments,” *Phys. Rev. A* **92**, 022709 (2015).
- [11] O. Thomas, C. Lippe, T. Eichert, and H. Ott, “Experimental realization of a Rydberg optical Feshbach resonance in a quantum many-body system,” *Nat. Comm.* **9**, 2238 (2018).
- [12] A. M. Kaufman, R. P. Anderson, T. M. Hanna, E. Tiesinga, P. S. Julienne, and D. S. Hall, “Radio-frequency dressing of multiple Feshbach resonances,” *Phys. Rev. A* **80**, 050701 (2009).
- [13] P. Zhang, P. Naidon, and M. Ueda, “Independent control of scattering lengths in multicomponent quantum gases,” *Phys. Rev. Lett.* **103**, 133202 (2009).
- [14] T. V. Tscherbul, T. Calarco, I. Lesanovsky, R. V. Krems, A. Dalgarno, and J. Schmiedmayer, “Rf-field-induced Feshbach resonances,” *Phys. Rev. A* **81**, 050701 (2010).
- [15] T. M. Hanna, E. Tiesinga, and P. S. Julienne, “Creation and manipulation of Feshbach resonances with radiofrequency radiation,” *New J. Phys.* **12**, 083031 (2010).
- [16] D. J. Papoular, G. V. Shlyapnikov, and J. Dalibard, “Microwave-induced Fano-Feshbach resonances,” *Phys. Rev. A* **81**, 041603 (2010).
- [17] D. H. Smith, “Inducing resonant interactions in ultracold atoms with a modulated magnetic field,” *Phys. Rev. Lett.* **115**, 193002 (2015).
- [18] D. J. Owens, T. Xie, and J. M. Hutson, “Creating Feshbach resonances for ultracold molecule formation with radio-frequency fields,” *Phys. Rev. A* **94**, 023619 (2016).
- [19] A. G. Sykes, H. Landa, and D. S. Petrov, “Two- and three-body problem with Floquet-driven zero-range interactions,” *Phys. Rev. A* **95**, 062705 (2017).
- [20] A. Guthmann, F. Lang, and A. Widera, “Engineering atomic interactions using Floquet-Feshbach resonances,” Preprint (2025).
- [21] D. H. Dunlap and V. M. Kenkre, “Dynamic localization of a charged particle moving under the influence of an electric field,” *Phys. Rev. B* **34**, 3625 (1986).
- [22] A. Eckardt, C. Weiss, and M. Holthaus, “Superfluid-insulator transition in a periodically driven optical lattice,” *Phys. Rev. Lett.* **95**, 260404 (2005).
- [23] H. Lignier, C. Sias, D. Ciampini, Y. Singh, A. Zenesini, O. Morsch, and E. Arimondo, “Dynamical control of matter-wave tunneling in periodic potentials,” *Phys. Rev. Lett.* **99**, 220403 (2007).
- [24] C. Sias, H. Lignier, Y. P. Singh, A. Zenesini, D. Ciampini, O. Morsch, and E. Arimondo, “Observation of photon-assisted tunneling in optical lattices,” *Phys. Rev. Lett.* **100**, 040404 (2008).
- [25] A. Zenesini, H. Lignier, D. Ciampini, O. Morsch, and E. Arimondo, “Coherent control of dressed matter waves,” *Phys. Rev. Lett.* **102**, 100403 (2009).
- [26] T. Salger, S. Kling, T. Hecking, C. Geckeler, L. Morales-Molina, and M. Weitz, “Directed transport of atoms in a Hamiltonian quantum ratchet,” *Science* **326**, 1241 (2009).
- [27] T. Kitagawa, E. Berg, M. Rudner, and E. Demler, “Topological characterization of periodically driven quantum systems,” *Phys. Rev. B* **82**, 235114 (2010).
- [28] S. E. Pollack, D. Dries, R. G. Hulet, K. M. F. Magalhães, E. A. L. Henn, E. R. F. Ramos, M. A. Caracanhas, and V. S. Bagnato, “Collective excitation of a Bose-Einstein condensate by modulation of the atomic scattering length,” *Phys. Rev. A* **81**, 053627 (2010).
- [29] J. Dalibard, F. Gerbier, G. Juzeliūnas, and P. Öhberg, “Colloquium: Artificial gauge potentials for neutral atoms,” *Rev. Mod. Phys.* **83**, 1523 (2011).
- [30] I. Vidanović, A. Balaž, H. Al-Jibbouri, and A. Pelster, “Nonlinear Bose-Einstein-condensate dynamics induced by a harmonic modulation of the  $s$ -wave scattering length,” *Phys. Rev. A* **84**, 013618 (2011).
- [31] J. Struck, C. Ölschläger, M. Weinberg, P. Hauke, J. Simonet, A. Eckardt, M. Lewenstein, K. Sengstock, and P. Windpassinger, “Tunable gauge potential for neutral and spinless particles in driven optical lattices,” *Phys. Rev. Lett.* **108**, 225304 (2012).
- [32] P. Hauke, O. Tieleman, A. Celi, C. Ölschläger, J. Simonet, J. Struck, M. Weinberg, P. Windpassinger, K. Sengstock, M. Lewenstein, and A. Eckardt, “Non-abelian gauge fields and topological insulators in shaken optical lattices,” *Phys. Rev. Lett.* **109**, 145301 (2012).
- [33] M. Aidelsburger, M. Atala, M. Lohse, J. T. Barreiro, B. Paredes, and I. Bloch, “Realization of the Hofstadter Hamiltonian with ultracold atoms in optical lattices,”

- Phys. Rev. Lett. **111**, 185301 (2013).
- [34] M. S. Rudner, N. H. Lindner, E. Berg, and M. Levin, “Anomalous edge states and the bulk-edge correspondence for periodically driven two-dimensional systems,” Phys. Rev. X **3**, 031005 (2013).
- [35] T. Wang, X.-F. Zhang, F. E. A. dos Santos, S. Eggert, and A. Pelster, “Tuning the quantum phase transition of bosons in optical lattices via periodic modulation of the  $s$ -wave scattering length,” Phys. Rev. A **90**, 013633 (2014).
- [36] N. Goldman and J. Dalibard, “Periodically driven quantum systems: Effective Hamiltonians and engineered gauge fields,” Phys. Rev. X **4**, 1 (2014).
- [37] G. Jotzu, M. Messer, R. Desbuquois, M. Lebrat, T. Uehlinger, D. Greif, and T. Esslinger, “Experimental realization of the topological Haldane model with ultracold fermions,” Nature **515**, 237 (2014).
- [38] W. Cairncross and A. Pelster, “Parametric resonance in Bose-Einstein condensates with periodic modulation of attractive interaction,” Europhys. J. D **68**, 106 (2014).
- [39] N. Fläschner, D. Vogel, M. Tarnowski, B. S. Rem, D. S. Lühmann, M. Heyl, J. C. Budich, L. Mathey, K. Senegstock, and C. Weitenberg, “Observation of dynamical vortices after quenches in a system with topology,” Nat. Phys. **14**, 1 (2017).
- [40] L. W. Clark, A. Gaj, L. Feng, and C. Chin, “Collective emission of matter-wave jets from driven Bose-Einstein condensates,” Nature **551**, 356 (2017).
- [41] N. Mann, M. Reza Bakhtiari, F. Massel, A. Pelster, and M. Thorwart, “Driven Bose-Hubbard model with a parametrically modulated harmonic trap,” Phys. Rev. A **95**, 043604 (2017).
- [42] B. Wang, F. N. Ünal, and A. Eckardt, “Floquet engineering of optical solenoids and quantized charge pumping along tailored paths in two-dimensional Chern insulators,” Phys. Rev. Lett. **120**, 243602 (2018).
- [43] A. J. E. Kreil, H. Y. Musienko-Shmarova, S. Eggert, A. A. Serga, B. Hillebrands, D. A. Bozhko, A. Pomyalov, and V. S. L’vov, “Tunable space-time crystal in room-temperature magnetodielectrics,” Phys. Rev. B **100**, 020406 (2019).
- [44] J. H. V. Nguyen, M. C. Tsatsos, D. Luo, A. U. J. Lode, G. D. Telles, V. S. Bagnato, and R. G. Hulet, “Parametric excitation of a Bose-Einstein condensate: From Faraday waves to granulation,” Phys. Rev. X **9**, 011052 (2019).
- [45] Z. Fedorova (Cherpakova), C. Jörg, C. Dauer, F. Letscher, M. Fleischhauer, S. Eggert, S. Linden, and G. von Freymann, “Limits of topological protection under local periodic driving,” Light Sci. & Appl. **8** (2019).
- [46] T. Wang, S. Hu, S. Eggert, M. Fleischhauer, A. Pelster, and X.-F. Zhang, “Floquet-induced superfluidity with periodically modulated interactions of two-species hardcore bosons in a one-dimensional optical lattice,” Phys. Rev. Res. **2**, 013275 (2020).
- [47] S. Fazzini, P. Chudzinski, C. Dauer, I. Schneider, and S. Eggert, “Nonequilibrium Floquet steady states of time-periodic driven Luttinger liquids,” Phys. Rev. Lett. **126**, 243401 (2021).
- [48] Z. Fedorova, C. Dauer, A. Sidorenko, S. Eggert, J. Kroha, and S. Linden, “Dissipation engineered directional filter for quantum ratchets,” Phys. Rev. Research **3**, 013260 (2021).
- [49] E. Wamba, A. Pelster, and J. R. Anglin, “Mapping as a probe for heating suppression in periodically driven quantum many-body systems,” arXiv:2108.07171 (2021).
- [50] D. Thuberg, S. A. Reyes, and S. Eggert, “Quantum resonance catastrophe for conductance through a periodically driven barrier,” Phys. Rev. B **93**, 180301 (2016).
- [51] S. A. Reyes, D. Thuberg, D. Pérez, C. Dauer, and S. Eggert, “Transport through an AC-driven impurity: Fano interference and bound states in the continuum,” New J. Phys. **19**, 043029 (2017).
- [52] D. Thuberg, E. Muñoz, S. Eggert, and S. A. Reyes, “Perfect spin filter by periodic drive of a ferromagnetic quantum barrier,” Phys. Rev. Lett. **119**, 267701 (2017).
- [53] F. Hübner, C. Dauer, S. Eggert, C. Kollath, and A. Sheikhan, “Floquet-engineered pair and single particle filter in the Fermi Hubbard model,” Phys. Rev. A **106**, 043303 (2022).
- [54] F. Hübner, C. Dauer, S. Eggert, C. Kollath, and A. Sheikhan, “Momentum-resolved Floquet-engineered pair and single-particle filter in the Fermi-Hubbard model,” Phys. Rev. A **108**, 023307 (2023).
- [55] K. Huang and C. N. Yang, “Quantum-mechanical many-body problem with hard-sphere interaction,” Phys. Rev. **105**, 767 (1957).
- [56] R. Stock, A. Silberfarb, E. L. Bolda, and I. H. Deutsch, “Generalized pseudopotentials for higher partial wave scattering,” Phys. Rev. Lett. **94**, 023202 (2005).
- [57] J. H. Shirley, “Solution of the Schrödinger equation with a Hamiltonian periodic in time,” Phys. Rev. **138**, B979 (1965).
- [58] H. Sambe, “Steady states and quasienergies of a quantum-mechanical system in an oscillating field,” Phys. Rev. A **7**, 2203 (1973).
- [59] M. Grifoni and P. Hänggi, “Driven quantum tunneling,” Phys. Rep. **304**, 229 (1998).
- [60] M. Holthaus, “Floquet engineering with quasienergy bands of periodically driven optical lattices,” J. Phys. B **49**, 013001 (2016).
- [61] A. Eckardt, “Colloquium: Atomic quantum gases in periodically driven optical lattices,” Rev. Mod. Phys. **89**, 1 (2017).
- [62] C. Brezinski, *History of continued fractions and Padé approximations* (Springer, Berlin, 1991).
- [63] C. Simmendinger, A. Wunderlin, and A. Pelster, “Analytical approach for the Floquet theory of delay differential equations,” Phys. Rev. E **59**, 5344 (1999).
- [64] D. Martinez, *Floquet theory and continued fractions for harmonically driven systems*, Ph.D. thesis, The University of Texas, Austin (2003).
- [65] U. Fano, “Effects of configuration interaction on intensities and phase shifts,” Phys. Rev. **124**, 1866 (1961).
- [66] A. E. Miroshnichenko, S. Flach, and Y. S. Kivshar, “Fano resonances in nanoscale structures,” Rev. Mod. Phys. **82**, 2257 (2010).
- [67] H. Friedrich and D. Wintgen, “Physical realization of bound states in the continuum,” Phys. Rev. A **31**, 3964 (1985).
- [68] H. Friedrich and D. Wintgen, “Interfering resonances and bound states in the continuum,” Phys. Rev. A **32**, 3231 (1985).
- [69] For the scalar product time averaging and space integration are used, so different Fourier components  $n \neq n'$  are orthogonal.



- [70] C. Dauer, “Resonances in interacting Floquet systems and dynamic transport phenomena,” Ph.D. Thesis, TU Kaiserslautern (2022).
- [71] A. M. Ishkhanyan, “Exact solution of the Schrödinger equation for the inverse square root potential  $v_0/\sqrt{x}$ ,” Europhys. Lett. **112**, 10006 (2015).

### End Matter A: Effective scattering amplitude

In order to derive Eq. (10) we apply Eq. (6) for  $n = \pm 1$

$$\begin{aligned} k_{\pm 1} f_{\pm 1} &= L_{\pm 1}(k_0 f_0 + k_{\pm 2} f_{\pm 2} - i) \\ &= L_{\pm 1}(k_0 f_0 + k_{\pm 1} f_{\pm 1} L_{\pm 2} g_{\pm 2}^{\pm} - i), \end{aligned} \quad (23)$$

where we have used  $g_{\pm 2}^{\pm} = k_{\pm 2} f_{\pm 2} / (L_{\pm 2} k_{\pm 1} f_{\pm 1})$ . Solving this for  $k_{\pm 1} f_{\pm 1}$  gives

$$\begin{aligned} k_{\pm 1} f_{\pm 1} &= L_{\pm 1}(k_0 f_0 - i) / (1 - L_{\pm 1} L_{\pm 2} g_{\pm 2}^{\pm}) \\ &= L_{\pm 1}(k_0 f_0 - i) g^{\pm}, \end{aligned} \quad (24)$$

where  $g^{\pm} = 1 / (1 - L_{\pm 1} L_{\pm 2} g_{\pm 2}^{\pm})$  are given by the continued fraction in Eq. (9) for  $n = \pm 1$ . For  $n = 0$  it follows from Eqs. (6) and (24) that

$$\begin{aligned} k_0 f_0 &= L_0(k_1 f_1 + k_{-1} f_{-1} - 2i\bar{a}/a_1) \\ &= L_0[(k_0 f_0 - i)(L_1 g^+ + L_{-1} g^-) - 2i\bar{a}/a_1] \\ &= 2L_0((k_0 f_0 - i)(a_s - \bar{a}) - i\bar{a})/a_1 \\ &= \frac{-k_0}{1 + ik_0 \bar{a}} [ik_0 f_0(a_s - \bar{a}) + a_s], \end{aligned} \quad (25)$$

where we have used Eq. (7) and defined

$$a_s - \bar{a} = a_1(L_1 g^+ + L_{-1} g^-)/2. \quad (26)$$

as in Eq. (11). Finally, solving Eq. (25) for  $f_0$  gives Eq. (10).

### End Matter B: Floquet Feshbach Resonance

The goal of this section is to evaluate the scattering contribution  $a_1 L_{-1} g^-$  from the closed channels in terms of the bound-state solutions  $|\phi^m\rangle$  and  $\epsilon_m$  as defined in Eqs. (13)–(15). The calculation leading to Eq. (11) defines the effective scattering length  $a_s$ , but we now use the ansatz that the bound Fourier modes  $\phi_{n<0}$  in Eq. (5) may be written as a superposition of orthonormal bound-state solutions  $|\phi^m\rangle$  in Eq. (13)

$$f_n \frac{e^{ik_n r}}{r} = \sum_m A_m \phi_n^m(r) \quad \text{for } n < 0. \quad (27)$$

In order to determine the expansion coefficients  $A_m$  we insert this ansatz into Eq. (4) and use the recursion relation in Eq. (14) to obtain

$$\sum_m (\epsilon - \epsilon_m) A_m \phi_n^m = \left[ \frac{\overleftarrow{\partial}}{\partial r} r \phi_0 \right] 2\pi a_1 \delta^3(\mathbf{r}) \delta_{n,-1}. \quad (28)$$

Here the double arrow indicates an hermitian operator acting both to the right and to the left [70], which becomes important when taking scalar products after multiplying both sides with  $\phi_n^{m'*}(r)$ . After integrating both sides [69], the orthonormality of solutions  $\sum_{n<0} \int d^3 \mathbf{r} \phi_n^{m'*}(r) \phi_n^m(r) = \delta_{m',m}$  gives

$$A_{m'} = \frac{2\pi a_1 D_{-1}^{m'*}}{\epsilon_{m'} - \epsilon} (1 + ik_0 f_0). \quad (29)$$

Finally, the relation  $k_{-1} f_{-1} = i \sum_m A_m D_{-1}^m$  from taking  $r \rightarrow 0$  in Eq. (27) can be inserted into Eq. (24), so that

$$L_{-1} g^- = - \sum_m \frac{2\pi a_1 |D_{-1}^m|^2}{\epsilon_m - \epsilon} \quad (30)$$

Following the analogous steps to Eq. (11) yields the important result Eq. (16) of the main text.

### End Matter C: Continuum limit

A continuum theory [19] can be defined in terms of a variable  $x = -n/A \geq 0$ , where we have rescaled the index according to

$$A = \left( \frac{a_1^2 \omega}{4} \right)^{1/3}, \quad \mathcal{D} \left( x = -\frac{n}{A} \right) = (-1)^n D_n. \quad (31)$$

Using  $D_{n+1} - 2D_n + D_{n-1} \approx \partial_x^2 \mathcal{D}(x)/A^2$  the bound state recursion relation in Eq. (14) becomes a differential equation

$$\left( -\frac{1}{\sqrt{x - \tilde{\epsilon}_m}} - \frac{\partial^2}{\partial^2 x} \right) \mathcal{D}(x) = -E \mathcal{D}(x), \quad (32)$$

$$\text{where} \quad E = 2A^2 \frac{1 - a_1}{a_1}. \quad (33)$$

Here we have used  $a_1 \kappa_n^m / (2A^2) = \sqrt{x - \tilde{\epsilon}_m}$  and defined  $\tilde{\epsilon}_m = \epsilon_m / (\omega A)$ . The rescaled Eq. (32) has only solutions for discrete dimensionless eigenvalues [71], which are given by  $E_m = 0.4380, 0.2632, 0.1976, 0.1617, 0.1386$  for the first five numerical solutions of  $\epsilon_m = 0$ . Inserting those values into Eq. (33) and solving for  $\omega$  we obtain the corresponding conditions for the resonant frequency for each solution

$$\omega_m = \frac{4}{a_1^2} \left( \frac{E_m}{2} \frac{a_1}{1 - a_1} \right)^{3/2}, \quad (34)$$

which shows a divergence as  $a_1 \rightarrow \bar{a}$ . Hence, the rescaling  $A$  also becomes quite large in that limit, which in turn justifies the continuous ansatz. The corresponding prefactor the continuum limit yields [70]

$$\Delta_m = \frac{F_m}{1 - a_1}, \quad (35)$$

where the first three coefficients are given by  $F_m = 0.212, 0.0628, 0.0313$ .